

Product Datasheet

HIF-1 alpha Antibody NB100-449

Unit Size: 0.1 ml

Store at 4C. Do not freeze.

www.novusbio.com



technical@novusbio.com

Reviews: 28 Publications: 286

Protocols, Publications, Related Products, Reviews, Research Tools and Images at:
www.novusbio.com/NB100-449

Updated 12/20/2023 v.20.1

**Earn rewards for product
reviews and publications.**

Submit a publication at www.novusbio.com/publications

Submit a review at www.novusbio.com/reviews/destination/NB100-449



NB100-449

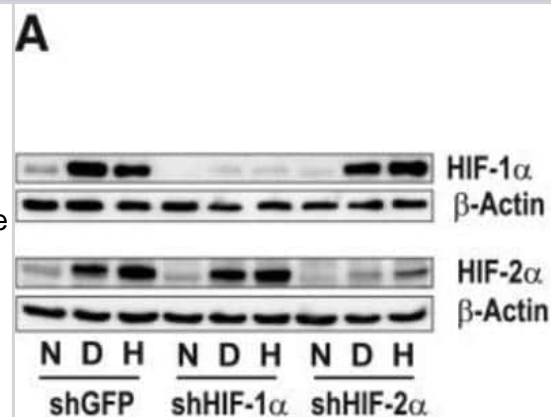
HIF-1 alpha Antibody

Product Information	
Unit Size	0.1 ml
Concentration	0.2 mg/ml
Storage	Store at 4C. Do not freeze.
Clonality	Polyclonal
Preservative	0.09% Sodium Azide
Isotype	IgG
Purity	Immunogen affinity purified
Buffer	TBS, 0.1% BSA
Target Molecular Weight	93 kDa
Product Description	
Host	Rabbit
Gene ID	3091
Gene Symbol	HIF1A
Species	Human, Mouse, Rat, Canine, Chicken, Goat, Primate, Monkey
Reactivity Notes	Monkey (COS-7) and Rat reactivities were reported in customer review feedback. Detection of HIF1 alpha in both Mouse and Human tissue by IHC. Chicken reactivity was reported in scientific literature (PMID: 25632022). Canine reactivity reported in scientific literature (PMID: 28701694). Reactivity with Goat is reported in PMID: 21599540.
Immunogen	The immunogen recognized by this HIF-1 alpha Antibody maps to a region between residues 775 and the C-terminus (residue 826) of human hypoxia-inducible factor 1 [Uniprot# Q16665].
Product Application Details	
Applications	Western Blot, Simple Western, ELISA, Flow Cytometry, Flow (Intracellular), Immunocytochemistry/ Immunofluorescence, Immunohistochemistry, Immunohistochemistry-Frozen, Immunohistochemistry-Paraffin, Immunoprecipitation, Chromatin Immunoprecipitation (ChIP), Knockdown Validated, Knockout Validated
Recommended Dilutions	Western Blot 1:2000 - 1:10000, Simple Western 1:200, Flow Cytometry 0.125 ug per 1 million cells in a 150 mcl reaction, ELISA 1:100-1:2000, Immunohistochemistry 1:100 - 1:500, Immunocytochemistry/ Immunofluorescence 1:10-1:500, Immunoprecipitation 2-5 ug/mg lysate, Immunohistochemistry-Paraffin 1:50-1:200, Immunohistochemistry-Frozen 1:50-1:200, Flow (Intracellular), Chromatin Immunoprecipitation (ChIP) 1:10-1:500, Knockout Validated, Knockdown Validated
Application Notes	ChIP usage was reported in scientific literature (PMID: 25557133). In Simple Western only 10 - 15 uL of the recommended dilution is used per data point. For IHC-P, Tris-EDTA pH 9.0 buffer is recommended for the heat induced epitope retrieval. ELISA (PMID: 17556599 and 16966370). Knockout data (PMID: 31793879). Use in Flow-intracellular reported in scientific literature (PMID:31722203).

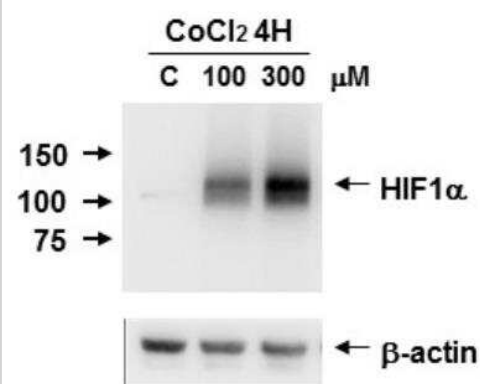


Images

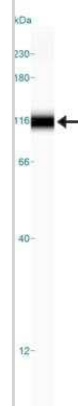
Knockdown Validated: HIF-1 alpha Antibody [NB100-449] - Morphological alterations induced by DMOG are HIF-1alpha dependent. gLIND.2 cells were stably transfected with shGFP, shHIF-1alpha or shHIF-2alpha. The clones were cultured under normoxic (N) or hypoxic (H, 1% O₂) conditions, or treated with DMOG for 6 h. 30 ug protein of cellular protein were loaded for the detection of HIF-1alpha, and nuclear extracts (20 ug protein) were used for the detection of HIF-2alpha. Image collected and cropped by CiteAb from the following publication (<https://biosignaling.biomedcentral.com/articles/10.1186/1478-811X-11-80>) licensed under a CC-BY license.



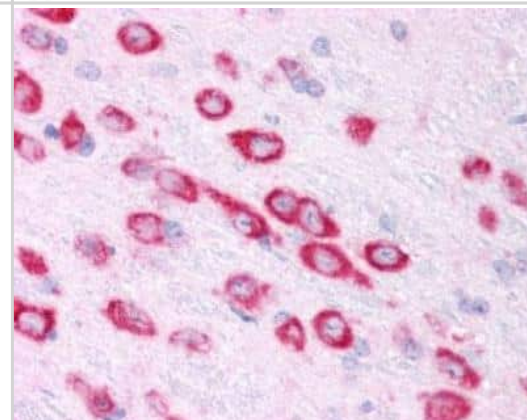
Western Blot: HIF-1 alpha Antibody [NB100-449] - HIF-1 alpha induction on Caki-1 cell lysate using CoCl₂. Image from verified customer review.



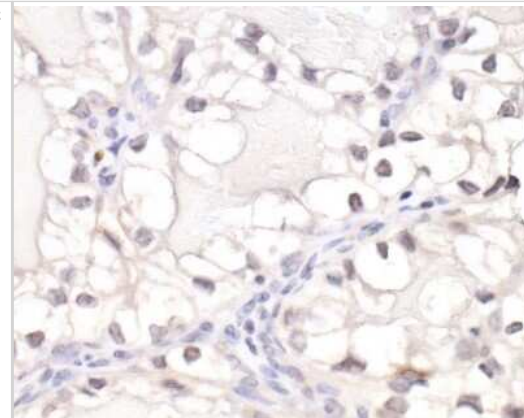
Simple Western: HIF-1 alpha Antibody [NB100-449] - Simple Western lane view shows a specific band for HIF-1 alpha in 0.5 mg/ml of hypoxic HeLa lysate. This experiment was performed under reducing conditions using the 12-230 kDa separation system.



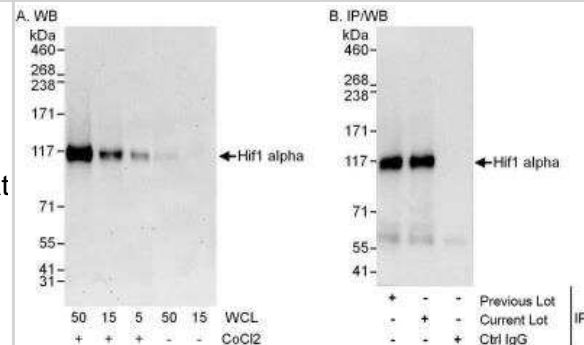
Immunohistochemistry: HIF-1 alpha Antibody [NB100-449] - Mouse Brain, Neurons 40X



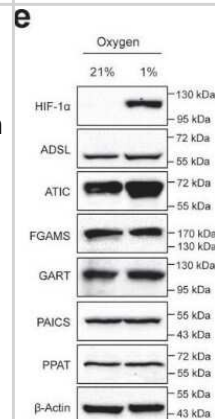
Immunohistochemistry: HIF-1 alpha Antibody [NB100-449] - Detection of human HIF1-alpha by immunohistochemistry. Sample: FFPE section of renal cell carcinoma. Antibody: Affinity purified rabbit anti-HIF1-alpha antibody (NB110-58773). Detection: DAB



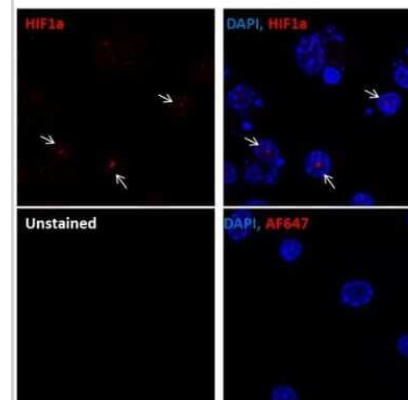
Western Blot: HIF-1 alpha Antibody [NB100-449] - Detection of Human HIF-1 alpha by Western Blot and Immunoprecipitation. Samples: Whole cell lysate (5, 15 and 50 ug for WB; 1 mg for IP, 20% of IP loaded) from HeLa cells that were either treated with cobalt chloride (+; 200 uM) or mock treated (-). Antibodies: Affinity purified rabbit anti-HIF1 alpha antibody used for WB at 0.1 ug/mL(A) and 1 ug/mL (B) and used for IP at 3 ug/mg lysate. HIF-1 alpha was also immunoprecipitated by a previous lot of this antibody. Detection: Chemiluminescence with exposure times of 30 seconds (A) and 10 seconds (B).



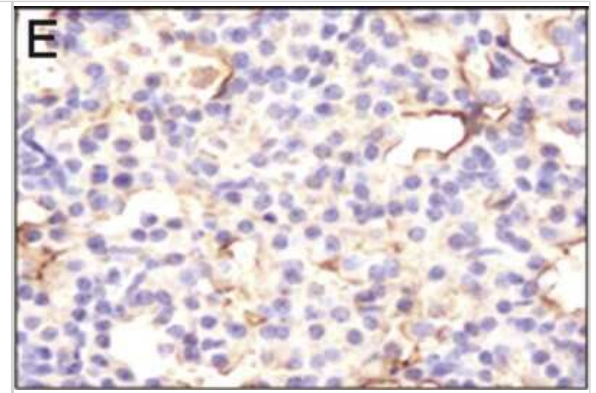
Western Blot: HIF-1 alpha Antibody [NB100-449] - Blot showing the effect of hypoxia on the protein expression levels of the purine biosynthetic enzymes. HIF-1 alpha is stabilized in hypoxia as expected, and no significant increase in the purine enzymes was detected between normoxic (21% oxygen) and hypoxic (1% oxygen) growth conditions. The positions of molecular markers surrounding each band of interest are shown for each blot. ADSL (NBP2-03107), ATIC (NBP2-01941), FGAMS (NBP1-84691), GART (H00002618-M01), HIF-1a (NB100-449), PAICS (NBP2-02817), PPAT (NBP2-02056). Image collected and cropped by CiteAb from the following publication (<https://pubmed.ncbi.nlm.nih.gov/32439803/>) licensed under a CC-BY license.



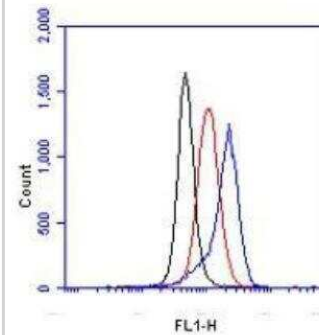
Immunocytochemistry/Immunofluorescence: HIF-1 alpha Antibody [NB100-449] - Murine primary bone marrow derived macrophages stained with HIF1-alpha antibody (red). Nuclei were counterstained with DAPI (blue). Image from verified customer review.



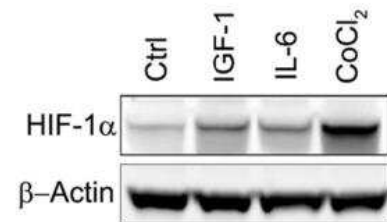
Immunohistochemistry-Paraffin: HIF-1 alpha Antibody [NB100-449] - Analysis of microvascular density and HIF-1alpha activity. Low, homogenous expression of HIF-1alpha was detected in the tumors of NNK treated mice (40X, scale bar = 25 um). Image collected and cropped by CiteAb from the following publication (<https://molecular-cancer.biomedcentral.com/articles/10.1186/1476-4598-11-4>), licensed under a CC-BY license.



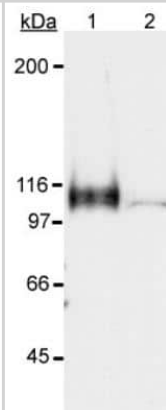
Flow Cytometry: HIF-1 alpha Antibody [NB100-449] - HeLa cells were treated for 15 hrs with 200 uM CoCl₂, fixed in PFA, and permeabilized in 90% MeOH. 1 X 10⁶ cells were stained with 0.125 ug anti-HIF-1 alpha and secondary FITC-conjugated goat anti-rabbit (in a 150 uL reaction). Black: treated, anti-KLH control IgG; Red: untreated, anti-HIF-1 alpha; Blue: treated, anti-HIF-1 alpha.



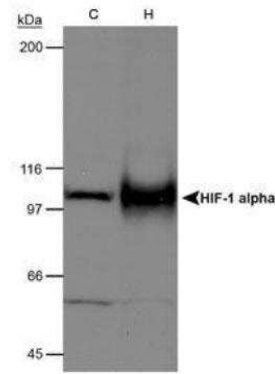
Western Blot: HIF-1 alpha Antibody [NB100-449] - Analysis of HIF-1 alpha in human myeloma cell lysate using anti-HIF-1 alpha. Cells were untreated or treated with IGF-1, IL-6 or CoCl₂. Image from verified customer review.



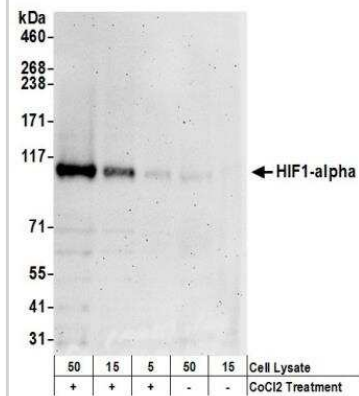
Western Blot: HIF-1 alpha Antibody [NB100-449] - Detection of HIF-1 alpha in a hypoxic sample. Lane 1: CoCl₂ treated Cos-7 nuclear extract (hypoxic). Lane 2: Untreated Cos-7 nuclear extract (normoxic).



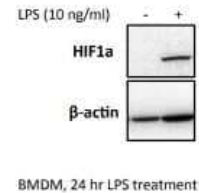
Western Blot: HIF-1 alpha Antibody [NB100-449] - Detection of mouse HIF-1 alpha on hypoxia treated MEFs



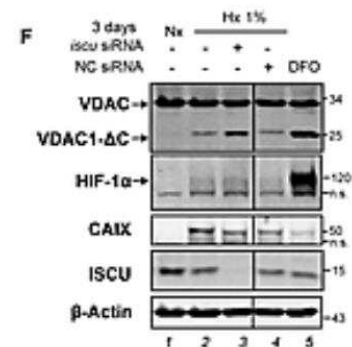
Western Blot: HIF-1 alpha Antibody [NB100-449] - Samples: Whole cell lysate (5, 15 and 50 ug) from HeLa cells that were treated with cobalt chloride (+; 200 uM) or mock treated (-). Antibodies: Affinity purified rabbit anti-HIF1 alpha antibody NB100-449 used for WB at 0.1 ug/ml. Detection: Chemiluminescence with exposure times of 30 seconds.



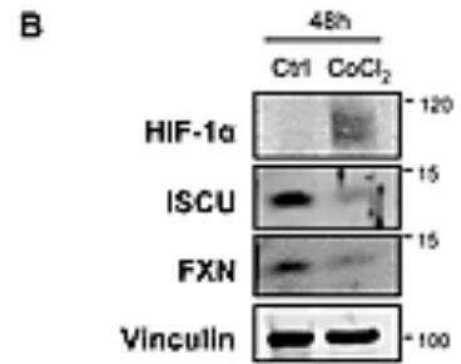
Western Blot: HIF-1 alpha Antibody [NB100-449] - BMDM were seeded at 0.5×10^6 overnight. Cells were treated with 10 ng/ml LPS for 24 hrs. Image from verified customer review.



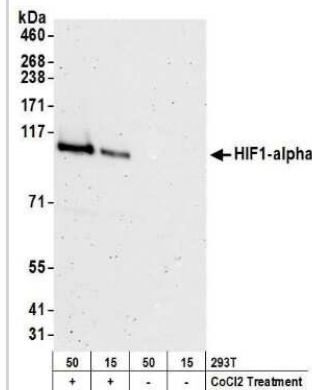
Western Blot: HIF-1 alpha Antibody [NB100-449] - Analysis of total protein using anti-HIF-1 alpha, -CAIX, -ISCU antibodies and VDACS antibody (PMID: 29596470).



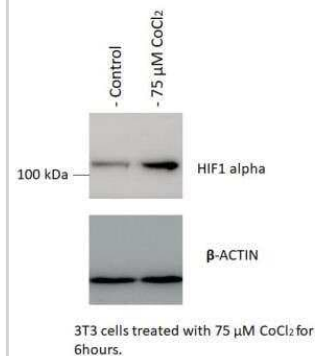
Western Blot: HIF-1 alpha Antibody [NB100-449] - Analysis of total protein using anti-HIF-1 alpha, -ISCU, -FXN antibodies. CoCl₂ was used to treat or not HeLa cells for 2 days (PMID: 29596470).



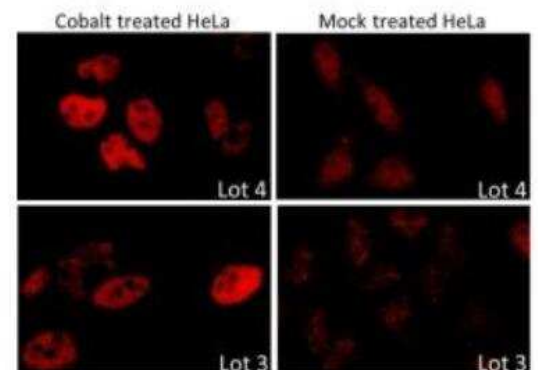
Western Blot: HIF-1 alpha Antibody [NB100-449] - Detection of human HIF1 alpha by western blot. Samples: Whole cell lysate (15 and 50 ug) from HEK293T cells that were either treated with 200 uM cobalt chloride (+) or mock treated (-). Antibodies: Affinity purified rabbit anti-HIF1 alpha antibody NB100-449 used for WB at 0.1 ug/ml. Detection: Chemiluminescence with exposure times of 3 minutes.



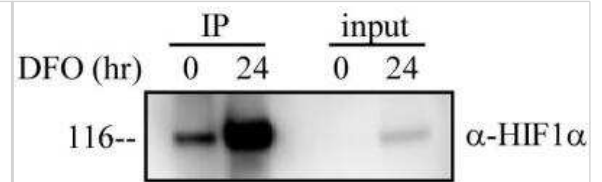
Western Blot: HIF-1 alpha Antibody [NB100-449] - 3T3-L1 mouse embryonic fibroblast adipose-like cell line. Antibody at 1:2000. WB image submitted by a verified customer review.



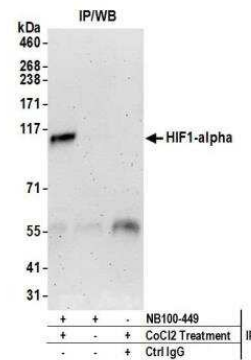
Immunocytochemistry/Immunofluorescence: HIF-1 alpha Antibody [NB100-449] - Formaldehyde-fixed asynchronous HeLa cells.



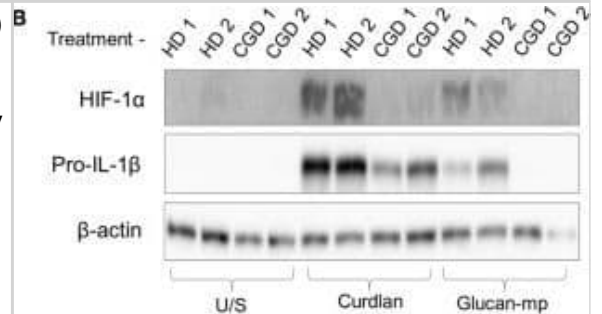
Immunoprecipitation: HIF-1 alpha Antibody [NB100-449] - HIF-1 alpha analysis in HEK293 cells. Image from verified customer review.



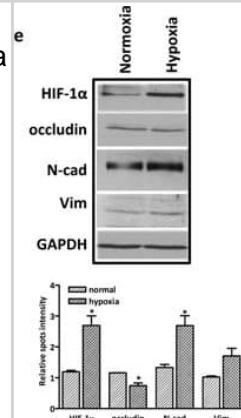
Immunoprecipitation: HIF-1 alpha Antibody [NB100-449] - Detection of human HIF1 alpha by western blot of immunoprecipitates. Samples: Whole cell lysate (1 mg for IP, 20% of IP loaded) from HEK293T cells that were treated with 200 μ M cobalt chloride. Antibodies: Affinity purified rabbit anti-HIF1 alpha antibody NB100-449 used for WB at 1 μ g/ml and for IP at 6 μ g/mg lysate. Detection: Chemiluminescence with exposure times of 3 minutes.



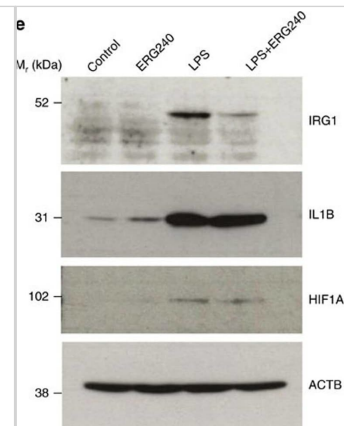
β -Glucan size affects the requirement for reactive oxygen species (ROS) in IL-1 β induction. (B) Human mDCs from healthy donors or chronic granulomatous disease (CGD) patients were stimulated with curdlan or glucan-mp for 8 h. HIF-1 α and pro-IL-1 β protein expression measured by immunoblot (n = 2 donors).



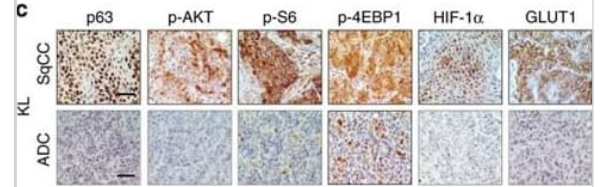
Hypoxia downregulates CFTR expression. (e) Western blot showing the expression changes of HIF-1alpha and EMT markers induced by hypoxia in MDCK cells, quantification analysis is shown in the lower panel, *p < 0.05; (Full-length blot is shown in Supplementary Figure S7d.). Image collected and cropped by CiteAb from the following publication (<https://pubmed.ncbi.nlm.nih.gov/28701694>), licensed under a CC-BY licence.



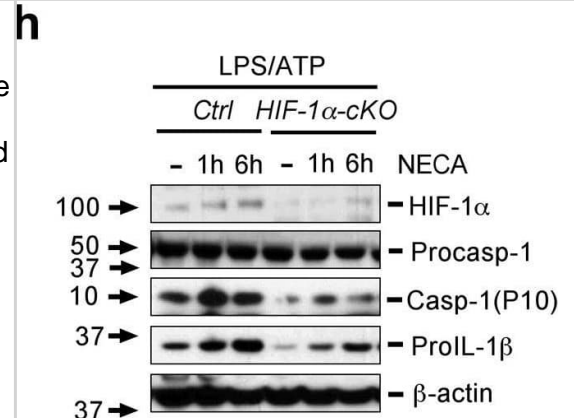
BCAT1 expression and inhibition in human macrophages. (e) Western blot analysis of IRG1, IL-1beta, HIF-1alpha and beta-actin (ACTB) in control (untreated), ERG240-treated (20 mM, 3 h), LPS treated (100 ng ml⁻¹, 3 h) and LPS+ERG240 treated (LPS, 100 ng ml⁻¹; ERG240, 20 mM for 3 h) hMDMs. The experiment is representative of three independent experiments using n=3 healthy donor hMDMs each. Image collected and cropped by CiteAb from the following publication (<https://www.nature.com/articles/ncomms16040>), licensed under a CC-BY licence.



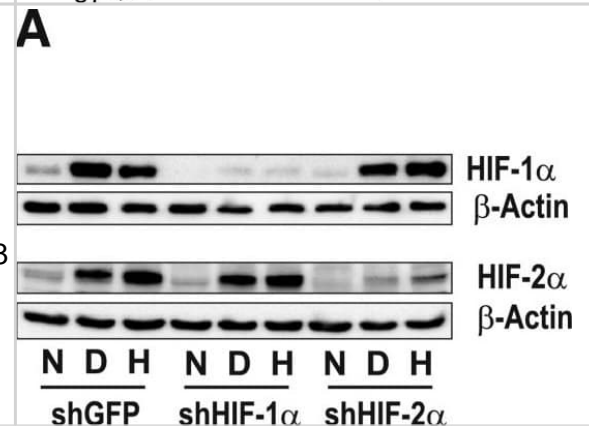
Elevated PIK3/AKT/HIF-1alpha pathways in KL SqCC tumours. (c) IHC analysis (top) and quantification (bottom) of p63, p-AKT, p-S6, p-4EBP1, HIF-1alpha and GLUT1 in KL tumours (n=6 each group). Two-tailed t-test, ****P<0.0001, ***P<0.001, **P<0.01. Scale bar, 50 um. Image collected and cropped by CiteAb from the following publication (<https://pubmed.ncbi.nlm.nih.gov/28548087>), licensed under a CC-BY licence.



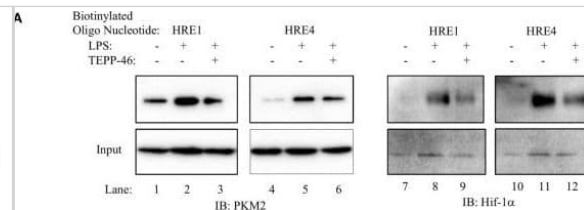
Adenosine mediates increase in pro-IL-1beta via a HIF-1alpha-dependent pathway. (h) LPS primed PECs obtained from HIF-1alpha-cKO and control mice were treated with or without NECA at different time points as indicated followed by pulsing with ATP. Cell lysates were collected after ATP pulsing. HIF-1alpha, pro-caspase-1, Caspase-1 and pro-IL-1beta was measured in cell supernatant by western blot. Immunoblots shown are representative results from at least three independent experiments. Image collected and cropped by CiteAb from the following publication (<https://pubmed.ncbi.nlm.nih.gov/24352507>), licensed under a CC-BY licence.



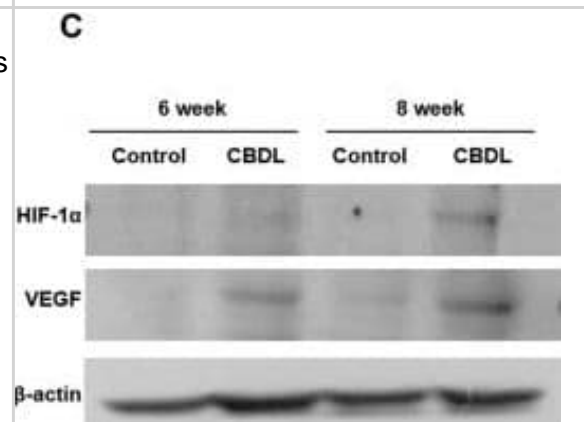
Morphological alterations induced by DMOG are HIF-1alpha dependent. (A) gIEND.2 cells were stably transfected with shGFP, shHIF-1alpha or shHIF-2alpha. The clones were cultured under normoxic (N) or hypoxic (H, 1% O₂) conditions, or treated with DMOG (D, 1 mM) for 6 h. 30 ug protein of cellular protein were loaded for the detection of HIF-1alpha, and nuclear extracts (20 ug protein) were used for the detection of HIF-2alpha. Image collected and cropped by CiteAb from the following publication (<https://biosignaling.biomedcentral.com/articles/10.1186/1478-811X-11-80>), licensed under a CC-BY licence.



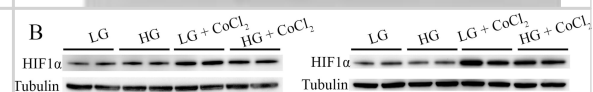
Pyruvate kinase isoform M2 (PKM2) and hypoxia-inducible factor 1alpha (Hif-1alpha) bind directly to the promoter region of PDL1 in primary murine BMDM cells. BMDM cells were treated with TEPP-46 at 50 uM for 1 h prior to stimulation with LPS (100 ng/ml, 24 h) (C) Sequential ChIP assays measuring simultaneous endogenous binding of PKM2 and Hif-1alpha to chromatin in response to LPS (100 ng/ml, 24 h) +/-TEPP-46 (pretreatment using 50 uM, 60 min). ChIP data are calculated as percent of input, error bar represents mean +/- SEM, and statistics are performed as two-tailed unpaired t-test *P < 0.05, **P < 0.01, and ***P < 0.001. Image collected and cropped by CiteAb from the following publication (<https://pubmed.ncbi.nlm.nih.gov/29081778>), licensed under a CC-BY licence.



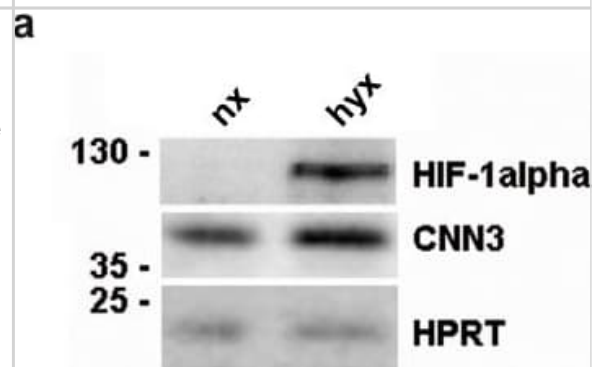
Changes in Hepatic Oxygen Saturation and Hypoxia-related Protein Expression. (C) In the Western blot analysis, the experimental group was relatively higher expression of hypoxia-inducible factor-1alpha (HIF-1alpha) and vascular endothelial growth factor (VEGF) protein than the control group at eight weeks. The full-length blots with these antibodies were presented in supplementary Figure S1. Image collected and cropped by CiteAb from the following publication (<https://pubmed.ncbi.nlm.nih.gov/29079853>), licensed under a CC-BY licence.



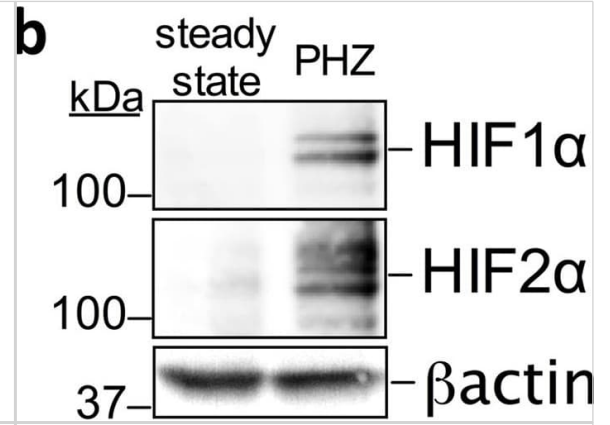
Effects of cell stress on VEGF-A and HIF1alpha expression in Muller cells and Y79 photoreceptors. (B) Western blots for HIF1alpha using cellular proteins, n = 4/group, ** p < 0.01. For MIO-M1 Muller cells: Grey bars: 5 mM glucose. Black bars: 25 mM glucose. For Y79 photoreceptors: Grey bars: 11 mM glucose. Black bars: 25 mM glucose. NS, not significant; LG, low glucose; HG, high glucose. Image collected and cropped by CiteAb from the following publication (<https://www.mdpi.com/1422-0067/18/3/533>), licensed under a CC-BY licence.



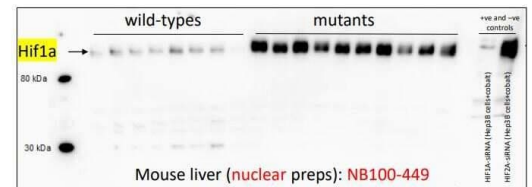
Hypoxic conditions upregulate CNN3 in BeWo cells. BeWo cells were cultured either under normoxic or under hypoxic conditions for 24hr. (A) Total protein lysates were examined with the Western Blot technique to detect CNN3 protein levels. For normalization, HPRT was stained on the same membrane. As hypoxia marker, HIF-1 alpha was detected as well. Image collected and cropped by CiteAb from the following publication (<https://pubmed.ncbi.nlm.nih.gov/25050546>), licensed under a CC-BY licence.



Phenylhydrazine administration results in hypoxia in retinal vessels and in HIF-1alpha and HIF-2alpha stabilization in peripheral blood leukocytes. (B) Representative analysis of HIFs by western blot: 50ug of protein from total cell lysate of blood leukocytes isolated from mice treated with PHZ compared to untreated. Image collected and cropped by CiteAb from the following publication (<https://pubmed.ncbi.nlm.nih.gov/28112274>), licensed under a CC-BY licence.

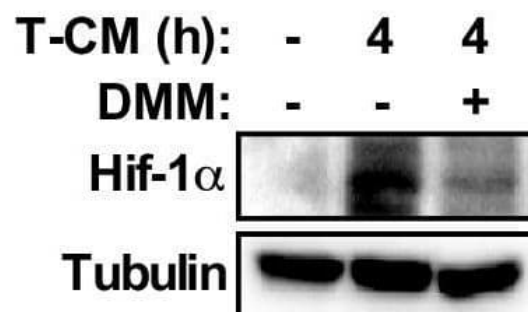


Western Blot: Rabbit Polyclonal HIF-1 alpha Antibody - Analysis of HIF-1 alpha antibody on mouse liver nuclear extracts. Image from a verified customer review.

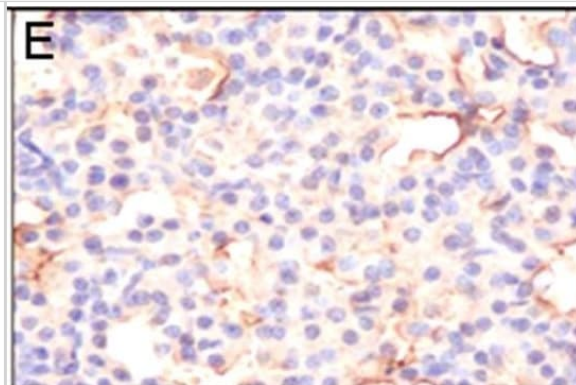


Improved survival and blood–brain barrier function post pneumococcal infection in mice by anti-HIF-1 α treatment using echinomycin. a Schematic depicting treatment protocol of mice infected with *S. pneumoniae* (D39). Mice were infected i.p., followed by anti-HIF-1 α treatment with echinomycin or just vehicle every 12 h starting 4 h post-infection (blue tick marks). Clinical scores were taken every 4 h starting 16 h post-infection (red line with tick marks) and study terminated at 48 h post-infection and brain tissues collected upon animal death or at the end point when the animals were sacrificed. b Clinical scores indicate improved symptoms in echinomycin-treated mice compared to vehicle-treated animals starting 16 h post-infection that were progression free (below score 1) up to 24 h (mean \pm SEM at each time, N = 10/group, ****p < 0.0001, **p < 0.01, *p < 0.05 by 2-tailed unpaired non-parametric Mann–Whitney t test at each time point. c Echinomycin-treated mice showed significantly improved overall survival percentage by Kaplan–Meier analysis with the median survival at 32 h compared to 25 h in vehicle-treated mice (**p < 0.01, log-rank test, N = 10/group). d Kaplan–Meier analysis also indicated a significant improvement in progression-free survival in echinomycin-treated animals (median survival 25 h) with no clinical symptoms up to 24 h (b) compared to the vehicle group (median survival 17 h; ***p < 0.001, log-rank test, N = 10/group). e Immunofluorescence staining for HIF-1 α , BBB permeability and junctional markers in the echinomycin and vehicle groups at the survival end point. Left panel shows that echinomycin treatment leads to a reduction in HIF-1 α -positive nuclei including in ECs co-stained for podocalyxin, a vascular marker which was unchanged by the treatment. Middle panel displays reduced vascular permeability to fibrinogen in the echinomycin group as indicated by stronger intravascular signal compared to the vehicle-treated mice. Increased expression of tight junction proteins—occludin (middle panel) and claudin-5 (right top panel)—in echinomycin-treated mice indicate improved BBB function. Tight junction-associated ZO-1, adherens junction marker VE-Cadherin, and endothelial cell adhesion molecule CD31 were unchanged (middle, bottom right panel). There was also no difference in *S. pneumoniae* (*Spn*) staining (right top panel) between the two groups. Scale bar 10 μ m. f Quantification of the staining from e utilizing four images per animal in the cortex region shows a significant reduction in HIF-1 α -positive cell number, whereas the total cell number or EC cell number was unchanged (left panel). As observed in e, the middle panel for quantification (arbitrary units—a.u.) of fibrinogen leakage shows significantly increased vascular staining for fibrinogen, supported by significantly increased expression of occludin, claudin-5, whereas other EC junction markers were unchanged. *S. pneumoniae* numbers in the vessels (v-*Spn*) or those transmigrated into brain parenchyma (b-*Spn*) were also unchanged. (mean \pm SEM, N = 7–10/group indicated by the corresponding number of dots, ****p < 0.0001, **p < 0.01, *p < 0.05 by 2-tailed unpaired Student's t test) Image collected and cropped by CiteAb from the following open publication (<https://pubmed.ncbi.nlm.nih.gov/32529267>), licensed under a CC-BY license. Not internally tested by Novus Biologicals.

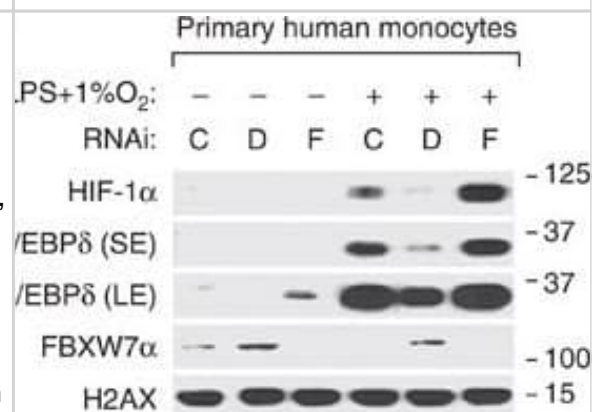
C



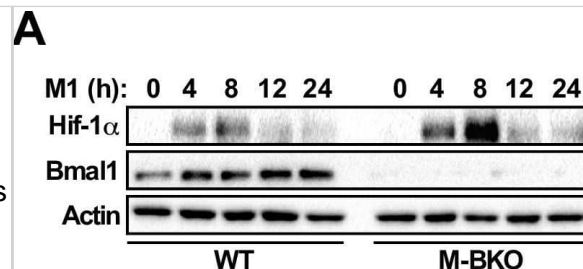
Compound MI-743 causes intracellular 8-oxo-dG accumulation and DNA damage. a MGC-803, HGC-27 and GES-1 cells were treated with DMSO or 5 μ M MI-743 for 48 h. Intracellular 8-oxo-dG was stained with Cy3-conjugated avidin. DNA was counterstained with 4,6-diamidino-2-phenylindole (DAPI). Images were acquired at $\times 100$ magnification by a Nikon Eclipse TE 2000-S fluorescence microscope. At least three independent experiments were performed for each group. b MGC-803, HGC-27 and GES-1 cells were treated with DMSO or 10 μ M MI-743 for 48 h and run in alkaline comet assay. Pictures were originally captured at $\times 40$ magnification. H₂O₂ was used as positive control. c Tail moment was calculated by CometScore software. Three individual experiments were performed for each group. d–f Western blot analysis of the protein levels of MTH1, MUTYH, OGG1, p21, ATMpS1981 and p53pS15 in MGC-803, HGC-27 and GES-1 cells, treated with increasing concentrations of MI-743 (0, 1, 2, 4, 8 and 12 μ M). g, h Densitometry shows relative protein expression normalized for GAPDH. Data are representative of three independent experiments. i–k Western Blot analysis of the protein levels of MTH1, MUTYH, OGG1, p21, ATMpS1981 and p53pS15 of protein lysates, isolated from MGC-803, HGC-27 and GES-1 cells, which were treated with 12 μ M MI-743 for 0, 12, 24, 36 and 48 h. l, m Densitometry shows relative protein expression normalized for GAPDH. Data are presented as means \pm SD. Three individual experiments were performed for each group. * $P < 0.05$, ** $P < 0.01$, *** $P < 0.001$ as compared with the controls Image collected and cropped by CiteAb from the following open publication (<https://pubmed.ncbi.nlm.nih.gov/31164636>), licensed under a CC-BY license. Not internally tested by Novus Biologicals.



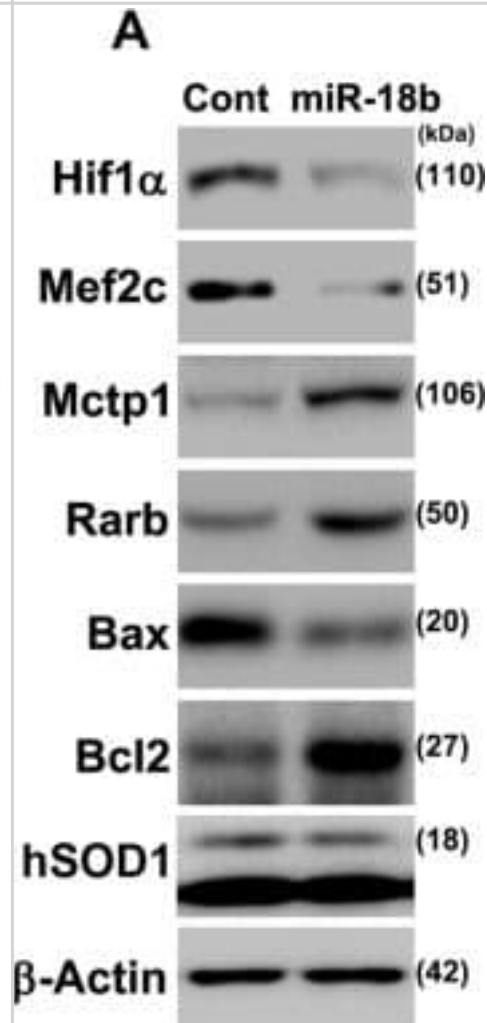
Successful knockdown of HIF-2 α in both 786-O and A498 renal cell lines. (A) Lysates from 786-O cells stably transfected with VHL (VHL +), parental 786-O cells (786-O), and 786-O cells infected with an empty retrovirus (pSuperRetro) or with retroviruses encoding single HIF-2 α shRNAs (HIF2 α shRNA 1; HIF2 α shRNA 2) or doubly infected with both shRNAs (HIF2 α shRNA 1+2) were immunoblotted for HIF-2 α (top panel), GLUT1 (upper middle panel) and VHL (lower middle panel). Bottom panel is an alpha tubulin immunoblot to demonstrate equal protein loading (25 μ g) in each lane. (B) Lysates from A498 cells stably transfected with VHL (VHL +), parental A498 cells (A498), and A498 cells infected with an empty retrovirus (pSuperRetro) or doubly infected with both HIF-2 α shRNAs (HIF2 α shRNA 1+2) were immunoblotted as in (A). Image collected and cropped by CiteAb from the following open publication (<https://pubmed.ncbi.nlm.nih.gov/17598890>), licensed under a CC-BY license. Not internally tested by Novus Biologicals.



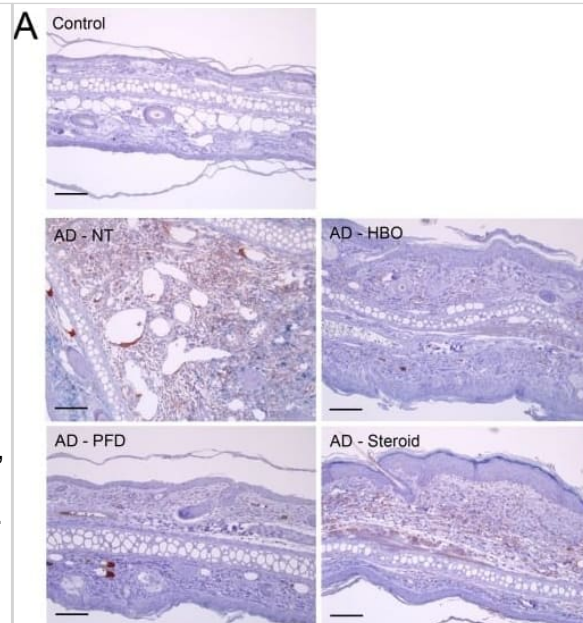
IQGAP1 induces the epithelial-to-mesenchymal transition, invasiveness, and proliferation of endometrial cancer (EC) cells. Reverse transcription quantitative PCR (qPCR) analysis of IQGAP1 mRNA in the immortalized human endometrial cell line EM and the EC cells HEC-1, HEC-50, and HEC-50-HI (HI). The results are presented as the fold-change in expression compared to the EM cells. B. Western blot analysis of the IQGAP1 protein in EC cells. C, E. The expression of IQGAP1, E-cadherin, and N-cadherin proteins in HI cells transfected with control (Ctr) or IQGAP1 siRNA (C) and in HEC-1 cells expressing either the control or IQGAP1 vector (E). D, F. Phase-contrast microscopy shows the morphology of HI cells transfected with control or IQGAP1 siRNA (D) and HEC-1 cells transfected with the control or IQGAP1 vector (F). G-I. Detection of migration (G), invasion (H), and proliferation (I) in HI and HEC-1 cells after the indicated transfection. J, K. qPCR analysis of ZO-1, CK-18, and Vimentin expression in HI (J) and HEC-1 (K) cells, transfected as indicated. L. Representative images from the invasion assays. Image collected and cropped by CiteAb from the following open publication (<https://www.oncotarget.com/lookup/doi/10.18632/oncotarget.7754>), licensed under a CC-BY license. Not internally tested by Novus Biologicals.



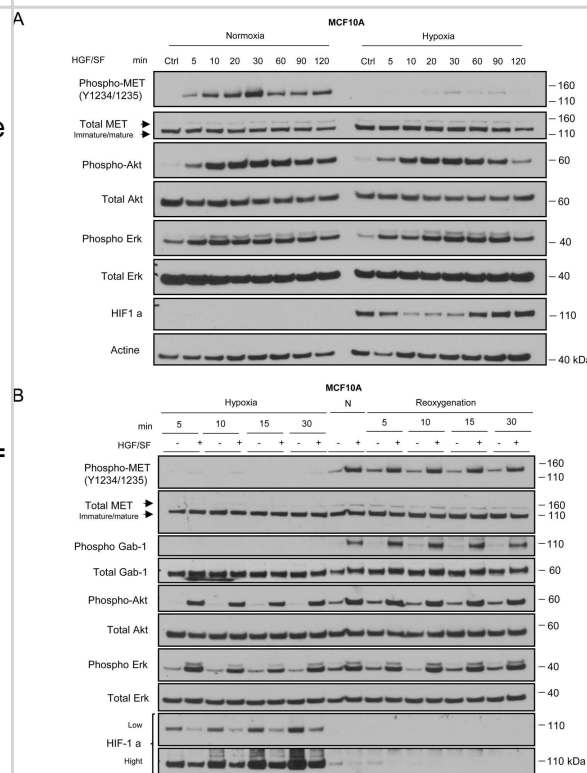
FDFT1 inhibits glycolysis through suppressing the AKT-mTOR-HIF1α pathway in CRC. aFDFT1 overexpression reduced glucose uptake in CT26 cells. bFDFT1 overexpression decreased lactate production via glycolysis in CT26 cells. c ECAR was reduced when FDFT1 was overexpressed in CT26 cells. d OCR was increased when FDFT1 was overexpressed in CT26 cells. eFDFT1 knockdown increased glucose uptake in CT26 cells. fFDFT1 knockdown increased lactate production via glycolysis in CT26 cells. g ECAR was increased when FDFT1 was knocked down in CT26 cells. h OCR was decreased when FDFT1 was knocked down in CT26 cells. i, mFDFT1 overexpression inhibited the protein and mRNA expression of mTOR-targeted glycolytic enzymes, including GLUT1, HK2, PGK1, GPI, and LDHA, in CT26 cells. j, mFDFT1 knockdown increased the protein and mRNA expression of mTOR-targeted glycolytic enzymes, including GLUT1, HK2, PGK1, GPI, and LDHA, in CT26 cells. k, nFDFT1 overexpression decreased the protein and mRNA expression of AKT, mTOR, and HIF1α. l, nFDFT1 knockdown increased the protein and mRNA expression of AKT, mTOR, and HIF1α. o Photograph of dissected tumors (the first line: normal diet, the second line: FMD + glucose, the third line: FMD, n = 5). p The tumor volumes were measured every 2 days after the 13th day. The FMD + glucose group can reverse the tumor growth inhibition induced by the FMD (n = 5; ns: P = 0.1838; P = 0.0001). q The protein level of FDFT1 and mTOR in dissected tumor samples from normal diet group, FMD group and FMD + glucose group was measured by western blotting. r The glucose level in these three groups. Error bars, mean ± SD, the data are from three independent experiments. Two-sided t tests. *P < 0.05, **P < 0.01, ***P < 0.001, compared with the control group (or normal diet group). #P < 0.05, ##P < 0.01. Image collected and cropped by CiteAb from the following open publication (<https://pubmed.ncbi.nlm.nih.gov/32313017>), licensed under a CC-BY license. Not internally tested by Novus Biologicals.



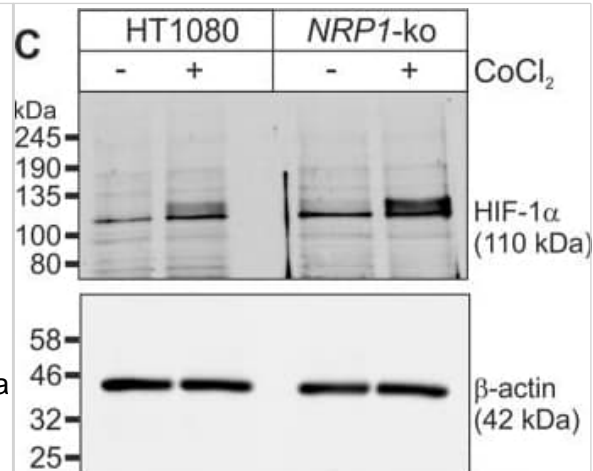
Effect of MLL-HCF1 interaction on histone methylation and Nrf2 expression in SNUC5/5-FUR cells. HCF1 expression was determined by Western blotting. *Significantly different from SNUC5 cells ($p < 0.05$). B. Interaction between MLL and HCF1 was examined by immunoprecipitation analysis using anti-MLL and anti-HCF1 antibodies followed by Western blotting with anti-HCF1 and anti-MLL antibodies. *Significantly different from SNUC5 cells ($p < 0.05$). C. Interaction between MLL and HCF1 was assessed by PLA. Each green spot represents for a single interaction (MLL and HCF1) and DNA was stained with DAPI. *Significantly different from SNUC5 cells ($p < 0.05$). The cells were transfected with non-targeting siRNA (siControl) or siHCF1 RNA for 24 h. D. Expression pattern of MLL mRNA in SNUC5/5-FUR cells was determined by RT-PCR analysis. *Significantly different from siControl-transfected cells ($p < 0.05$). E. Expression pattern of HCF1, MLL, and Nrf2 in SNUC5/5-FUR cells was determined by Western blot analysis. *Significantly different from siControl-transfected cells ($p < 0.05$). Image collected and cropped by CiteAb from the following open publication (<https://www.oncotarget.com/lookup/doi/10.18632/oncotarget.9745>), licensed under a CC-BY license. Not internally tested by Novus Biologicals.



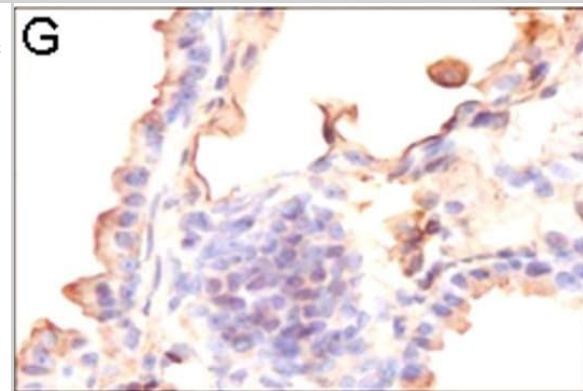
Induction of ubiquitin/proteasome-dependent DSBs in CPT-treated quiescent WI38 hTERT cells. (A–F) Serum-starved cells were treated with DMSO (1 h) or with MG132 (50 μ M, 1 h), lactacystin (10 μ M, 1 h), bortezomib (1 μ M, 4 h), G5 (1.5 μ M, 0.5 h) or Pyr-41 (9 μ M, 0.5 h) before the addition of DMSO (untreated) or 25 μ M CPT for 1 h and then co-stained for γ H2AX (green) and 53BP1 (red) or analyzed by Western blot. ‘-’ in panels C and F means cells treated with DMSO. (A and D) Representative pictures. Nuclear contours, identified by DAPI staining (not shown), are indicated by dashed lines. Bars: 10 μ m. (B and E) Number of γ H2AX foci per nucleus from two independent experiments (147–153 nuclei were analyzed for each treatment). **** $P < 0.0001$. (C and F) Western blot of γ H2AX. α Tubulin: loading control. Dashed lines indicate that intervening wells have been spliced out. The top panels show quantification of γ H2AX normalized to α Tubulin (means \pm SEM, $n = 4$ in panel C, $n = 3$ in panel F). *** $P < 0.001$; ** $P < 0.01$. (G and H) Detection of DSBs by neutral Comet assays in serum-starved cells treated with DMSO or MG132 (25 μ M) for 1 h before the addition of DMSO (untreated) or CPT for 1 h (7.5 μ M for experiments (Exp I and II; 5 and 7.5 μ M for Exp III). (G) Representative pictures of nuclei from Exp I. (H) Quantification of neutral Comet tail moments for three independent experiments (95–133 nuclei were analyzed for each treatment in each experiment). *** $P < 0.001$; **** $P < 0.0001$. The untreated and CPT data from Exp I are from the same experiment as that of Supplementary Figure S3D. Image collected and cropped by CiteAb from the following open publication (<https://pubmed.ncbi.nlm.nih.gov/26578593>), licensed under a CC-BY license. Not internally tested by Novus Biologicals.



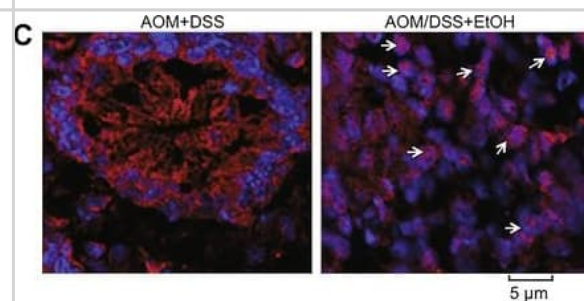
S100A7 is secreted and acts as a chemotactic factor of cell migration and invasion. Cells were cultured in serum-free medium for 2 days, then the medium was collected, fractionated, followed by Western Blot analysis. B&C. Transwell migration and Matrigel invasion assays were performed in C33A and SiHa cells. Cell suspension was placed into the upper chamber in 0.1 ml of DMEM serum-free medium, and conditioned medium from S100A7-overexpressed C33A and SiHa cells and their corresponding control cells was placed in the lower chamber as a chemoattractant. The stained cells were manually counted from 4 randomly selected fields and normalized with cell proliferation [2-sided t test; * $P < 0.05$; *** $P < 0.001$]. Representative image and quantitative results of cell migration and invasion were shown (B. C33A cells; C. SiHa cells; $\times 10$, bars:100 μm). Image collected and cropped by CiteAb from the following open publication (<https://www.oncotarget.com/lookup/doi/10.18632/oncotarget.15329>), licensed under a CC-BY license. Not internally tested by Novus Biologicals.



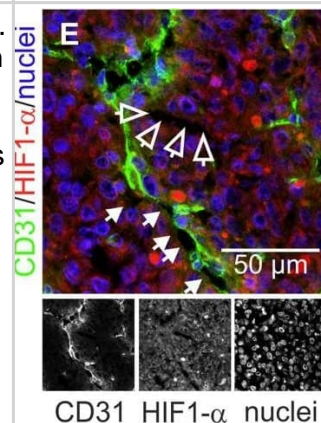
Increased expression of HIF α and/or Twist in A549 and H441 cells induced by the inhibition of PIMT and Thapsigargin(A) Immunoblotting of Slug, ZEB1, Snail1, Twist, and HIF1 α in A549 sh-PIMT and sh-control cells. (B, C) Immunoblotting and relative intensity of HIF1 α in A549 cells treated with Tg. (D) Immunoblotting of Slug, ZEB1, Snail1, Twist, and HIF1 α in si-control cells and si-PIMT H441 cells. (E, F) Immunoblotting and relative intensity of HIF1 α in H441 cells treated with Tg. #1 and #2 indicates si-RNA of J-010000-05-0002 and J-010000-07-0002, respectively. Image collected and cropped by CiteAb from the following open publication (<https://www.oncotarget.com/lookup/doi/10.18632/oncotarget.24324>), licensed under a CC-BY license. Not internally tested by Novus Biologicals.



Characterization of CIP2A expression in a panel of normal human melanocytes (NHM) and melanoma cell lines. (A) Immunoblot analysis and (B) quantification of protein expression levels of CIP2A (C) CIP2A mRNA expression measured by qRT-PCR. NHM1 line was used as calibrator. (D) Cytoplasmic and nuclear expression of CIP2A in normal melanocytes, primary and metastatic melanoma cell lines assessed by immunoblot analysis and (E) by immunohistochemical staining. CIP2A, cancerous inhibitor of protein phosphatase 2A. Image collected and cropped by CiteAb from the following open publication (<https://pubmed.ncbi.nlm.nih.gov/25663244>), licensed under a CC-BY license. Not internally tested by Novus Biologicals.



Role of inflammasome in glucose fluctuation-induced myocardial fibrosis. (A) Immunofluorescence staining of intracellular NLRP3–ASC interaction examined by confocal microscopy. The NRCFs were labeled with anti-NLRP3 (red), anti-ASC (green), and DAPI (blue) (n = 3 per group). (B–G) After siRNA targeting NLRP3 transfection, the protein expressions of NLRP3, cleaved caspase-1 and collagen I were measured by western blot (n = 3 per group). (H) Representative images of immunofluorescence staining of intracellular α -SMA in the NG, HG, GF, and GF + siRNA groups (n = 3 per group). Image collected and cropped by CiteAb from the following open publication (<https://pubmed.ncbi.nlm.nih.gov/35592403>), licensed under a CC-BY license. Not internally tested by Novus Biologicals.



Publications

□korja Mili? N, Dolinar K, Mi□ K et al. Suppression of Pyruvate Dehydrogenase Kinase by Dichloroacetate in Cancer and Skeletal Muscle Cells Is Isoform Specific and Partially Independent of HIF-1? International Journal of Molecular Sciences 2021-08-10 [PMID: 34445316] (WB)

Tiwari R, Bommi PV, Gao P et al. Chemical inhibition of oxygen-sensing prolyl hydroxylases impairs angiogenic competence of human vascular endothelium through metabolic reprogramming iScience 2022-10-21 [PMID: 36157579] (Func)

Gobelli D, Serrano-Lorenzo P, Esteban-Amo MJ et al. The mitochondrial succinate dehydrogenase complex controls the STAT3-IL-10 pathway in inflammatory macrophages iScience 2023-08-18 [PMID: 37575201]

Prieto-Fern□ndez E, Egia-Mendikute L, Bosch A et al. Hypoxia Promotes Syndecan-3 Expression in the Tumor Microenvironment Frontiers in Immunology 2020-09-30 [PMID: 33117401] (WB)

Moreno-Loshuertos R, Movilla N, Marco-Brualla J et al. A Mutation in Mouse MT-ATP6 Gene Induces Respiration Defects and Opposed Effects on the Cell Tumorigenic Phenotype International Journal of Molecular Sciences 2023-01-09 [PMID: 36674816] (FLOW)

Marrocco A, Frawley K, Pearce LL et al. Metabolic Adaptation of Macrophages as Mechanism of Defense against Crystalline Silica The Journal of Immunology 2021-09-15 [PMID: 34433619] (ICC/IF)

Pirkmajer S, Bezjak K, Matkovi? U et al. Ouabain Suppresses IL-6/STAT3 Signaling and Promotes Cytokine Secretion in Cultured Skeletal Muscle Cells Frontiers in Physiology 2020-09-25 [PMID: 33101052]

Sil S, Singh S, Chemparathy DT et al. Astrocytes & Astrocyte derived Extracellular Vesicles in Morphine Induced Amyloidopathy: Implications for Cognitive Deficits in Opiate Abusers Aging and disease 2021-09-01 [PMID: 34527417]

Laquatra C, Sanchez-Martin C, Dinarello A et al. HIF1?-dependent induction of the mitochondrial chaperone TRAP1 regulates bioenergetic adaptations to hypoxia Cell Death & Disease 2021-05-01 [PMID: 33934112]

Noonan ML, Ni P, Solis E et al. Osteocyte EglN1/Phd2 links oxygen sensing and biomineralization via FGF23 Bone Research 2023-01-18 [PMID: 36650133] (WB)

Deval G, Nedder M, Degrelle S et al. Benzo(a)pyrene and Cerium Dioxide Nanoparticles in Co-Exposure Impair Human Trophoblast Cell Stress Signaling International journal of molecular sciences 2023-03-12 [PMID: 36982514] (IHC-P, Human)

Details:

Dilution: 1:500

Tsai HC, Tong ZJ, Hwang TL et al. Acrolein produced by glioma cells under hypoxia inhibits neutrophil AKT activity and suppresses anti-tumoral activities Free radical biology & medicine 2023-07-04 [PMID: 37414347] (IHC, Mouse)

More publications at <http://www.novusbio.com/NB100-449>

Procedures

Immunohistochemistry Protocols (NB100-449)

IHC - Frozen 7 um mouse frozen sections were used.

Detection system: Vectors Anti-Rabbit Ig ImmPRESS Reagent Kit (cat # MP-7401)

1. Fix in ice cold acetone
2. Block for one hour at room temp. The block is provided by the vector kit; it is 2.5% horse serum.
3. Use NB 100-449 at a 1:100 dilution in PBS and incubate overnight in the fridge.
4. Perform a 15 min peroxidase block and incubated with the ImmPress anti-rabbit for 30 mins at RT.
5. Use DAB to detect staining and counterstained with Vectors Hemotoxylin. PBS washes (3X2 mins) were done in between all steps except in between the block and the primary

IHC-FFPE sections

I. Deparaffinization:

- A. Treat slides with Xylene: 3 changes for 5 minutes each. Drain slides for 10 seconds between changes.
- B. Treat slides with 100% Reagent Alcohol: 3 changes for 5 minutes each. Drain slides for 10 seconds between changes.

II. Quench Endogenous Peroxidase:

To Prepare 200 ml of Quenching Solution:

Add 3 ml of 30% Hydrogen Peroxide to 200 ml of Methanol.

**Use within 4 hours of preparation

- A. Place slides in peroxidase quenching solution: 15-30 minutes.
- B. Place slides in distilled water: 2 changes for 2 minutes each.

III. Retrieve Epitopes:

- A. Preheat Citrate Buffer. Place 200 ml of Citrate Buffer Working Solution into container, cover and place into steamer. Heat to 90-96C.
- B. Place rack of slides into hot Citrate Buffer for 20 minutes. Cover.
- C. Carefully remove container with slides from steamer and cool on bench, uncovered, for 20 minutes.
- D. Slowly add distilled water to further cool for 5 minutes.
- E. Rinse slides with distilled water, 2 changes for 2 minutes each

IV. Immunostaining Procedure:

- A. Remove each slide from rack and circle tissue section with a hydrophobic barrier pen (e.g. Liquid Blocker-Super

Pap Pen).

B. Flood slide with Wash Solution.

Do not allow tissue sections to dry for the rest of the procedure.

C. Drain wash solution and apply 4 drops of Blocking Reagent to each slide and incubate for 15 minutes.

D. Drain Blocking Reagent (do not wash off the Blocking Reagent), apply 200 ul of Primary Antibody solution to each slide, and incubate for 1 hour.

E. Wash slides with Wash Solution: 3 changes for 5 minutes each.

F. Drain wash solution, apply 4 drops of Secondary antibody to each slide and incubate for 1 hour.

G. Wash slides with Wash Solution: 3 changes for 5 minutes each.

H. Drain wash solution, apply 4 drops of DAB Substrate to each slide and develop for 5-10 minutes.

Check development with microscope.

I. Wash slides with Wash Solution: 3 changes for 5 minutes each.

J. Drain wash solution, apply 4 drops of Hematoxylin to each slide and stain for 1-3 minutes. Increase time if darker counterstaining is desired.

K. Wash slides with Wash Solution: 2-3 changes for 2 minutes each.

L. Drain wash solution and apply 4 drops of Bluing Solution to each slide for 1-2 minutes.

M. Rinse slides in distilled water.

N. Soak slides in 70% reagent alcohol: 3 minutes with intermittent agitation.

O. Soak slides in 95% reagent alcohol: 2 changes for 3 minutes each with intermittent agitation.

P. Soak slides in 100% reagent alcohol: 3 changes for 3 minutes each with intermittent agitation. Drain slides for 10 seconds between each change.

Q. Soak slides in Xylene: 3 changes for 3 minutes each with intermittent agitation. Drain slides for 10 seconds between each change.

R. Apply 2-3 drops of non-aqueous mounting media to each slide and mount coverslip.

S. Lay slides on a flat surface to dry prior to viewing under microscope.

NOTES:

-Use treated slides (e.g. HistoBond) to assure adherence of FFPE sections to slide.

-Prior to Deparaffinization, heat slides overnight in a 60C oven.

-All steps in which Xylene is used should be performed in a fume hood.

-For Epitope Retrieval, a microwave or pressure cooker may be substituted for the steamer method. Adjust times as necessary depending on conditions.

-For the initial IHC run with a new primary antibody, test tissues with and without Epitope Retrieval. In some instances, Epitope Retrieval may not be necessary.

-200 ul is the recommended maximum volume to apply to a slide for full coverage. Using more than 200 ul may allow solutions to wick off the slide and create drying artifacts, for small tissue sections less than 200 ul may be used.

-5 minutes of development with DAB Substrate should be sufficient. Do not develop for more than 10 minutes. If 5 minutes of development causes background staining, further dilution of the primary antibody may be necessary.

-Hematoxylin should produce a light nuclear counterstain so as not to obscure the DAB staining. Counterstain for 1-1.5 minutes for nuclear antigens. Counterstain for 2-3 minutes for cytoplasmic and membranous antigens. If darker counterstaining is desired increase time (up to 10 minutes)





Novus Biologicals USA

10730 E. Briarwood Avenue
Centennial, CO 80112
USA
Phone: 303.730.1950
Toll Free: 1.888.506.6887
Fax: 303.730.1966
nb-customerservice@bio-techne.com

Bio-Techne Canada

21 Canmotor Ave
Toronto, ON M8Z 4E6
Canada
Phone: 905.827.6400
Toll Free: 855.668.8722
Fax: 905.827.6402
canada.inquires@bio-techne.com

Bio-Techne Ltd

19 Barton Lane
Abingdon Science Park
Abingdon, OX14 3NB, United Kingdom
Phone: (44) (0) 1235 529449
Free Phone: 0800 37 34 15
Fax: (44) (0) 1235 533420
info.EMEA@bio-techne.com

General Contact Information

www.novusbio.com
Technical Support: nb-technical@bio-techne.com
Orders: nb-customerservice@bio-techne.com
General: novus@novusbio.com

Products Related to NB100-449

NBP2-36452	HeLa Hypoxic / Normoxic Cell Lysate
HAF008	Goat anti-Rabbit IgG Secondary Antibody [HRP]
NB7160	Goat anti-Rabbit IgG (H+L) Secondary Antibody [HRP]
NBP2-24891	Rabbit IgG Isotype Control

Limitations

This product is for research use only and is not approved for use in humans or in clinical diagnosis. Primary Antibodies are guaranteed for 1 year from date of receipt.

For more information on our 100% guarantee, please visit www.novusbio.com/guarantee

Earn gift cards/discounts by submitting a review: www.novusbio.com/reviews/submit/NB100-449

Earn gift cards/discounts by submitting a publication using this product:
www.novusbio.com/publications

